arXiv:cond-mat/0608534v5 [cond-mat.mtrl-sci] 6 May 2009

Temperature dependent Electron Landé g-Factor and Interband Matrix Element in GaAs

J. Hübner,* S. Döhrmann, D. Hägele,† and M. Oestreich
Institute for Solid State Physics, Gottfried Wilhelm Leibniz Universität Hannover, Appelstr. 2, 30167 Hannover, Germany
(Dated: March 23, 2022)

Very high precision measurements of the electron Landé g-factor in GaAs are presented using spin-quantum beat spectroscopy at low excitation densities and temperatures ranging from 2.6 to 300 K. In colligation with available data for the temperature dependent effective mass a temperature dependence of the interband matrix element within a common five level $\mathbf{k}\cdot\mathbf{p}$ -theory can model both parameters consistently. A strong decrease of the interband matrix element with increasing temperature consistently closes a long lasting gap between experiment and theory and substantially improves the modeling of both parameters.

PACS numbers: 78.55.Cr,78.47.Cd,78.20.Ci,71.18.+y

The semiempirical $\mathbf{k}\cdot\mathbf{p}$ - theory is a universal tool to calculate the band structure in semiconductors and semiconductor heterostructures and is regularly employed in such different fields as the physics of semiconductor laser design, the quantum Hall effect, and spintronics. The part of the theory describing magnetic field related phenomena has been extensively improved since its introduction by Kane [1], Luttinger and Kohn [2] in the mid fifties. Nowadays, 5- and more band $\mathbf{kp}$ - models are state of the art and many low temperature experiments have confirmed the incredible accuracy of $\mathbf{k}\cdot\mathbf{p}$ - calculations [3, 4, 5, 6, 7, 8]. All these experiments support the validity of $\mathbf{kp}$ - theory whereas a single but central experiment, which measures the temperature dependence of the electron Landé g-factor in GaAs, shows a strong discrepancy between experiment and $\mathbf{k}\cdot\mathbf{p}$ - theory [9].

In this paper we present extremely high precision, temperature dependent measurements of the electron Landé g-factor and show that by introducing a temperature dependent interband matrix element yields a consistent explanation for the temperature dependence of the electron Landé g-factor and the effective mass within common $\mathbf{k}\cdot\mathbf{p}$ -theory, while keeping full temperature dependence on the very well known interband critical points. The $\mathbf{k}\cdot\mathbf{p}$ - theory is a perturbation theory calculating the electronic band-structure by expansion around a single point in the Brillouin zone. In direct semiconductors like GaAs, the high symmetry Γ-point is the natural expansion point. The only input parameters are in this case the measured band-gaps at $\mathbf{k} = 0$ and the interband matrix elements $(P, P', P'', \ldots)$. The change of the band-gap energies with the lattice temperature are very well known for GaAs and the only remaining relevant parameter which does not possess a direct experimental access is the interband matrix element P or the related Kane energy $E_P = (2m_0/\hbar^2)P^2$, respectively [1]. The temperature dependence of P has been assumed to be marginal since P is inversely proportional to the interatomic distance a [10] and the well known change of a with temperature T due to anharmonic lattice potential is small. According to the relation $E_P \propto 1/a^2$ between 0 K and 300 K E_P should change about -0.4% or less [11, 12]. However, this procedure only considers the static change of $1/a^2$. With a phenomenological approach of a temperature dependency of E_P the experimental data can only be correctly described by an about 14 times larger, i.e., -5.4% decrease of E_P from 2.6 K to room temperature.

The sample used in the experiment is bulk GaAs grown by molecular beam epitaxy with a donor concentration of $1.2 \cdot 10^{15}\,\mathrm{cm}^{-3}$. The temperature dependent electron Landé g-factor is measured by spin-quantum-beat spectroscopy in the following way: The sample is mounted in Voigt geometry in a split coil superconducting magnet and excited with circular polarized light pulses from an 80 MHz picosecond laser. The sample temperature is varied from 2.6 K to room temperature, whereas the excess-energy of the exciting light is about 6 meV above the direct band gap for temperatures up to 80 K. At higher temperatures, the contribution of the excess energy is negligible compared to the thermal energies present in the sample lattice. The excited carrier density is $6 \cdot 10^{15}\,\mathrm{cm}^{-3}$. The photoluminescence from the sample is collected in backward direction. Energy- and time-resolution are performed by a spectrometer followed by a synchroscan streak camera. The electron Landé g-factor is deduced from the oscillating time evolution of the cross circular polarized component of the photoluminescence via the relation $g^* = \omega_L\hbar/(\mu_B B)$, with ω_L being the Larmor precession frequency of the conduction electron spins, μ_B Bohr's magneton, and B the magnetic field.

Great care has been taken in the time calibration of the detection system as well as in the correct determination of the magnetic field present in the superconducting magnet. Superconducting magnets can often show unapparent remanence fields and incorrect field calibrations which easily influence the experimental data. Therefore the magnetic field is calibrated with a precise Hall sensor for all applied fields. The often cited value of $g^* = -0.44(2)$ [13] in GaAs applies for donor bound

electrons, whereas for the free conduction band electrons higher absolute g-factor values are reported [14, 15]. From the data presented here, a very high accuracy extrapolated electron Landé g-factor of $g^* = -0.484(3)$ at $T = 0\,\mathrm{K}$, $B = 0\,\mathrm{T}$, and $P_{\mathrm{exc.}} = 0\,\mathrm{mW}$ is determined.

Figure 1 shows the electron Landé g-factor versus sample temperature. Each value is extrapolated to zero magnetic field and zero excitation power from measurements at different fields [16] and excitation powers at constant temperature to eliminate any residual effects of those entities on the g-factor. The measurements from 2.6 to 62 K are carried out with alternating excitation of left and right circular polarized light and a small tilt of the sample against the magnetic field. This technique enables us to monitor and subtract the influence of the effective nuclear field on the electron Landé g-factor measurement (see Ref. [17] for details). This procedure is especially at low temperatures much more precise concerning the absolute value of g^* than compared with other techniques like e.g. Ref. [18].

Next the experimental results are compared with established 5-level **kp** - theory [19]. Cardona was the first to suggest a 5-level approach based on the wavefunction expansion of the isoelectric group IV counterpart [4]. However, the central 5-level $\mathbf{k}\cdot\mathbf{p}$ - result for g^* and m^* used in this work was put forward by Hermann *et al.* [8] with P and P' as free parameters:

$$\frac{g^*}{g_0} = 1 - \frac{E_P}{3}\left(\frac{1}{E(\Gamma_6^c-\Gamma_8^v)} - \frac{1}{E(\Gamma_6^c-\Gamma_7^v)}\right) - \frac{E_{P'}}{3}\left(\frac{1}{E(\Gamma_7^c-\Gamma_6^c)} - \frac{1}{E(\Gamma_8^c-\Gamma_6^c)}\right) + \Delta_{\mathrm{so}}^g + C' \quad (1)$$

$$\frac{m_0}{m^*} = 1 + \frac{E_P}{3}\left(\frac{2}{E(\Gamma_6^c-\Gamma_8^v)} + \frac{1}{E(\Gamma_6^c-\Gamma_7^v)}\right) - \frac{E_{P'}}{3}\left(\frac{1}{E(\Gamma_7^c-\Gamma_6^c)} + \frac{2}{E(\Gamma_8^c-\Gamma_6^c)}\right) + \Delta_{\mathrm{so}}^m + C \quad (2)$$

Here, $g_0 = 2.0023$ is the free electron Landé g-factor, m_0 the free electron mass, and $E(\Gamma_7^v, \Gamma_8^v, \Gamma_6^c, \Gamma_7^c, \Gamma_8^c)$ are the energies of the band extrema at the center of the Brillouin zone. The correction Δ_{so}^g due to the spin orbit coupling $\bar{\Delta} = -50\,\mathrm{meV}$ [20] between the valence and higher conduction band has a significantly strong contribution to the electron Landé g-factor [6, 21] and is given by:

$$\Delta_{\mathrm{so}}^g = -\frac{2}{9}\bar{\Delta}\sqrt{E_P E_{P'}}\left(\frac{2}{E(\Gamma_6^c-\Gamma_7^v)\cdot E(\Gamma_7^c-\Gamma_6^v)} + \frac{1}{E(\Gamma_6^c-\Gamma_8^v)\cdot E(\Gamma_8^c-\Gamma_6^v)}\right) \quad (3)$$

Further corrections by $\bar{\Delta}$ to the terms linear in $E_{P,P'}$ in Eqs. 1 and 2 change g^* below 0.1% and are neglected. The corresponding correction for the effective mass Δ_{so}^m is included in the calculation as well, but has a much smaller effect on the calculation of m^* than Δ_{so}^g has on g^*. The contributions from higher bands are summarized

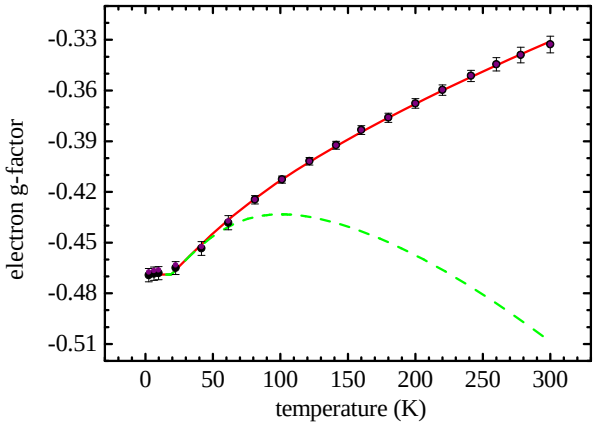


FIG. 1: (Color online) High precision measurement of the temperature dependence of the electron Landé g-factor in bulk GaAs (filled circles). The red solid line is a fit of the experimental data by Eq. 1 with a strong temperature dependent interband matrix element. The green dashed line is the calculated g^* with $E_P(T)$ depending only on the anharmonic lattice expansion. Both calculations contain both the dilatational and electron-phonon contribution to the change in the interband critical points according to Eqn. 4 and values shown in Tab. I.

in the constants $C' = -0.021$ and $C = -1.878$ taken from Ref. [7].

The spin orbit interaction results mainly from contributions of the atomic species in the material which is in good approximation temperature independent. The temperature dependence of the band-gap energies $E(T)$ are very well known for GaAs by experiment and described by the semi-phenomenological model introduced by Viña et al. [22] collecting the electron and phonon dynamics in one context:

$$E(T) = E_B - \alpha_B\left(1 + \frac{2}{e^{\Theta/T}-1}\right). \quad (4)$$

This model is used for all following calculations, but nearly identical results are obtained by using the popular empirical relation by Varshni [23]. The parameters for the $\mathbf{k}\cdot\mathbf{p}$ - calculations are listed in Tab. I.

Equation 1 yields the electron Landé g-factor at the conduction band minimum. At finite temperatures, the known energy dependence of the electron Landé g-factor $g^*(E) = g^* + 6.3\,\mathrm{eV}^{-1}\cdot E$ on the kinetic energy E of the electrons in GaAs (Ref. [5], Fig. 7) is included by weighting g^* with the thermal distribution [24] of the electrons in the conduction bands:

$$\langle g^*\rangle = \frac{\int_0^\infty dE\, g^*(E)\, D^{3\mathrm{D}}(E)\, e^{\frac{-E}{k_{\mathrm{B}}T_{\mathrm{e}}}}}{\int_0^\infty dE\, D^{3\mathrm{D}}(E)\, e^{\frac{-E}{k_{\mathrm{B}}T_{\mathrm{e}}}}}. \quad (5)$$

The integration starts at the minimum of the conduction band, $D^{3\mathrm{D}}(E) = {}^1\!/_{2\pi^2}\left({}^{2\,m^*}\!/_{\hbar^2}\right)^{3/2}\sqrt{E}$ is the three-dimensional density of states, k_{B} Boltzmann's constant,

TABLE I: Parameters used

	E_B eV	α_B meV	Θ K	Ref.
$E(\Gamma_6^c - \Gamma_8^v)$	1.571 eV	57	240	[a]
$E(\Gamma_6^c - \Gamma_7^v)$	1.907 eV	58	240	[a],[b]
$E(\Gamma_7^c - \Gamma_8^v)$	4.563 eV	59	323	[a]
$E(\Gamma_8^c - \Gamma_8^v)$	4.718 eV	59	323	[c],[d]
E_P	28.9 eV	914	240	[e],[f]
$E_{P'}$	6.1 eV	914	240	[e],[f],[g]

[a] from Ref. [25].
[b] The value for α for the Varshni model in [25] contains a typing error. It should read $\alpha = 5.4 \cdot 10^{-4}$ eV/K as seen from the data presented.
[c] from Ref. [8]. Here $\alpha_B = 59$ meV has been added to E_B to account for the Viña model used in this work.
[d] Assumption that the temperature dependence of the $E(\Gamma_8^c)$ is the same as for the $E(\Gamma_7^c)$ band due to the lack of available data. The induced error is small, since these values contribute only weakly to the g-factor correction.
[e] Given by the value of g^* and m^* at T=0 K.
[f] The ratio of E_P and $E_{P'}$ compares to that estimated by Cardona *et al.* [4, 21]. Note that $E_P(T)[[\text{eV}]] = (2m_0/\hbar^2)(P^{(')}[\text{eV m}])^2(T)$.
[g] Assumption that the temperature dependence of E_P is the same as for the $E_{P'}$. See also [d].

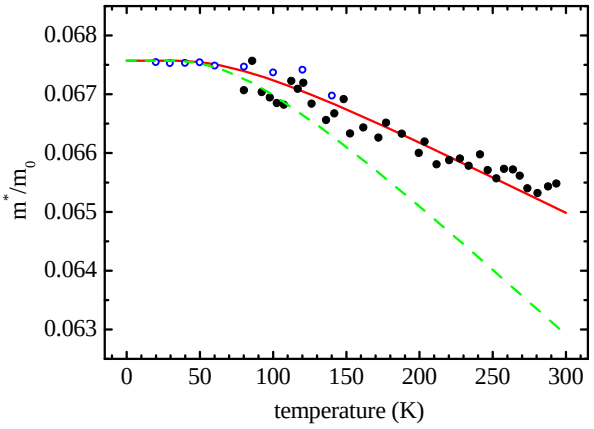


FIG. 2: (Color online) Temperature dependence of the effective conduction electron mass in bulk GaAs (hollow blue circles [5], full black circles [26]). The red solid line follows Eq. 1 with a strong temperature dependent interband matrix. The green dashed line is calculated with the conventional temperature dependence of E_P. Please note the different impact of E_P on g^* and m^* acc. to Eq. 1 and 2.

and T_e the effective electron temperature. The temperature dependence of the effective conduction band mass m^* has been taken into account in D^{3D} according to Eq. 2. At lattice temperatures T_L below 20 K, the effective electron temperature T_e is constant due to the excess energy of the optical excitation and phase space filling. At higher lattice temperatures, the electron-phonon coupling is much more efficient and T_e is in good approximation equal to the lattice temperature, and phase space filling can be neglected for the calculation of $\langle g^* \rangle$ due to the low excitation densities.

The green dashed line in Fig. 1 shows $\langle g^* \rangle$ calculated with Eq. 5 including the weakly temperature dependent interband matrix element due to the anharmonic lattice potential alone evincing that the model is in clear disagreement with the measurements. In the next step, additionally the same temperature relation for the Kane energies, i.e., the interband matrix elements is assumed as for the band-gap energies in Eq. 4 and the linear prefactor α_B is the *only* fit parameter, keeping Θ fixed to 240 K. The resulting red solid line in Fig. 1 exhibits excellent agreement with the measurement. This fit however implies that the interband matrix element reduces from helium to room temperature by as much as -5.4% within this model and can not be explained by the tiny average lattice expansion expected from the anharmonic lattice potential alone.

To substantiate the possibility of a strong temperature dependence of the interband matrix elements, the experimentally determined temperature dependence of the effective mass in GaAs is compared with predictions by the same 5-level $\mathbf{k}\cdot\mathbf{p}$ - model. Figure 2 shows the temperature dependent effective mass of GaAs measured by cyclotron resonance [5] and magneto-phonon [26] spectroscopy. The data presented from these publications represent the 'bare' effective mass at the conduction band minimum (cf. [27]). The red solid line in Fig. 2 depicts the calculated temperature dependence of m^* (Eq. 2) including the strong dependency of the interband matrix elements on the temperature according to Eq. 4. Only parameters consistently obtained with the g^*-data according to Tab. I are employed, i.e., the calculation of m^* has *no* free parameter. Nevertheless the calculation is in excellent agreement with the experiment, whereas the discrepancy between conventional $\mathbf{k}\cdot\mathbf{p}$ - theory and experiment is obvious: The green dashed line in Fig. 2 shows the same calculation but with the old established temperature dependence of the interband matrix elements.

We want to illustrate a semiclassical possible physical origin of a stronger temperature dependence of P. The presence of longitudinal acoustical phonons creates a locally and temporally varying conduction band energy leading to electronic states with lowered energy via the deformation potential distributed over a range of phonon wavelengths corresponding to the occupancy of the phonon energies. Similarly, hole states with higher energies appear in the band structure. Note that the fraction of the well known band gap shrinkage due to electron-phonon interaction with elevated temperatures is treated differently [28, 29]. For phonon wavelengths longer than the electron scattering length the free conduction band electrons are fast compared to the lattice dynamics and can follow the local, phonon-induced conduction band minima adiabatically on small scales. As a consequence the electrons average preferentially over

elongated lattice sites and the wavefunction overlap between conduction and valence band states, i.e., the interband matrix element is reduced. The mean square relative displacement for all occupied longitudinal acoustic phonon branches is easily calculated and yields a reduction of E_P by -0.4 % at 100 K and -1.6 % at 300 K compared to 0 K. This estimated shrinkage is already a factor of four bigger than the established shrinkage due to the anharmonicity of the lattice potential. Modeling the temperature dependence of g^* and m^* can be as well pursued by inserting only the dilatational part of the interband critical points instead of taking into account the full temperature dependence of the interband critical points and matrix elements. Due to the smaller contribution of the dilatational part to the interband critical points, their change is less strong than the full change in the optical gap and the result is mathematically nearly identical compared to the approach following Eqns. 1 and 2. The concept of the effective mass band gap E_g^* [30] would accordingly be extended to the "effective electron Landé g-factor band gap" in this work. However, both concepts cannot be distinguished within the same $\mathbf{k}\cdot\mathbf{p}$-description employed here and the full temperature behavior of the interband critical points is much more precisely known, than their change with lattice constant, i.e their pressure dependence. Nevertheless both effects can yield a contribution at the same time, especially since electron-phonon interaction has a small but non vanishing contribution affecting the band curvature [31]. The contemplations involving the dynamical change in interatomic distances like those pointed out above for E_P should be included in future analyses to improve on the modeling of the central quantities of the employed 5-level $\mathbf{k}\cdot\mathbf{p}$-model.

In summary, the electron Landé g-factor in GaAs has been determined with very high precision in dependence on the sample temperature resulting in a free conduction band g-factor of $-0.484(3)$ at T=0 K. The experimental data on the temperature dependence of g^* and m^* have been consistently modeled with a modified $\mathbf{k}\cdot\mathbf{p}$-formalism. We suggest to include phonon induced lattice fluctuations similar to the band gap shrinkage of semiconductors, which support the experimental findings.

The authors thank Roland Winkler for helpful discussions and appreciate H.J. Queisser's inspiration. The work is founded by the German Science Foundation (DFG - Priority Program 1285 "Semiconductor Spintronics"), the Federal Ministry for Education and Research (BMBF - Program NanoQUIT) and QUEST Hannover.

* Electronic address: jhuebner@nano.uni-hannover.de
† Now at: Spectroscopy of Condensed Matter, Ruhr-Universität Bochum, 44801 Bochum, Germany

[1] E. O. Kane, J. Phys. Chem. Sol. **1**, 249 (1957).
[2] J. M. Luttinger and W. Kohn, Phys. Rev. **97**, 869 (1955).
[3] L. Roth, B. Lax, and S. Zwerdling, Phys. Rev. **114**, 90 (1959).
[4] M. Cardona, J. Phys. Chem. Solids **24**, 1543 (1963).
[5] M. Hopkins, R. Nicholas, P. Pfeffer, W. Zawadzki, D. Gauthier, J. Portal, and M. DiForte-Poisson, Semicond. Sci. Technol. **2**, 568 (1987).
[6] P. Pfeffer and W. Zawadzki, Phys. Rev. B **41**, 1561 (1990).
[7] H. Mayer and U. Rössler, Phys. Rev. B **44**, 9048 (1991).
[8] C. Hermann and C. Weisbuch, Phys. Rev. B **15**, 823 (1977).
[9] M. Oestreich and W. W. Rühle, Phys. Rev. Lett. **74**, 2315 (1995).
[10] M. Cardona, *Atomic Structure and Properties of Solids*, p. 514 (Academic Press, New York, 1972).
[11] L. G. Shantharama, A. R. Adams, C. N. Ahmad, and R. J. Nicholas, Journal of Physics C: Solid State Physics **17**, 4429 (1984).
[12] P. Lawaetz, Phys. Rev. B **4**, 3460 (1971).
[13] C. Weisbuch and C. Hermann, Phys. Rev. B **15**, 816 (1977).
[14] M. Krapf, G. Denninger, H. Pascher, G. Weimann, and W. Schlapp, Solid State Commun. **74**, 1141 (1990).
[15] M. Schreiner, H. Pascher, G. Denninger, S. A. Studenikin, G. Weimann, and R. Lösch, Solid State Commun. **102**, 715 (1997).
[16] Measurements at magnetic fields ranging from 0.3 to 7 Tesla enter into the extrapolation.
[17] S. Döhrmann, S. Oertel, D. Hägele, J. Hübner, and M. Oestreich, to be publ. (2009).
[18] P. E. Hohage, G. Bacher, D. Reuter, and A. D. Wieck, Appl. Phys. Lett. **89**, 231101 (2006).
[19] Recent higher order $\mathbf{k}\cdot\mathbf{p}$ - models [32] certainly give more accurate results for e.g. the magnetic Luttinger parameter but they yield even with some improvements [33] only a poor description of the electron Landé g-factor [34].
[20] H. Sigg, J. A. A. J. Perenboom, P. Pfeffer, and W. Zawadzki, Solid State Commun. **61**, 685 (1987).
[21] M. Cardona, N. E. Christensen, and G. Fasol, Phys. Rev. B **38**, 1806 (1988).
[22] L. Viña, S. Logothetidis, and M. Cardona, Phys. Rev. B **30**, 1979 (1984).
[23] Y. P. Varshni, Physica (Utrecht) **34**, 149 (1967).
[24] The need to account for a redistribution effects resulting from Landau levels as pursued in Ref. [35] is circumvented here by extrapolation to zero magnetic field.
[25] P. Lautenschlager, M. Garriga, S. Logothetidis, and M. Cardona, Phys. Rev. B **35**, 9174 (1987).
[26] H. Hazama, T. Sugimasa, T. Imachi, and C. Hamaguchi, J. Phys. Soc. Jpn. **55**, 1282 (1986).
[27] R. A. Stradling and R. A. Wood, J. Phys. C: Solid State Phys. **1**, 1711 (1968).
[28] H. Y. Fan, Phys. Rev. **82**, 900 (1951).
[29] P. B. Allen and V. Heine, J. Phys. C **9**, 2305 (1976).
[30] H. Ehrenreich, J. Phys. Chem. Solids **2**, 131 (1957).
[31] H. Fröhlich, H. Pelzer, and S. Zienau, Phil. Mag. **41**, 221 (1950).
[32] S. Richard, F. Aniel, and G. Fishman, Phys. Rev. B **70**, 235204 (2004).
[33] N. Fraj, S. Ben Radhia, and K. Boujdaria, Solid State Commun. **142**, 342 (2007).
[34] F. Nastos, R. W. Newson, J. Hübner, H. M. van Driel, and J. E. Sipe, Phys. Rev. B **77**, 195202 (2008).
[35] K. L. Litvinenko, L. Nikzad, C. R. Pidgeon, J. Allam,

L. F. Cohen, T. Ashley, M. Emeny, W. Zawadzki, and B. N. Murdin, Phys. Rev. B **77**, 033204 (2008).